0026-895X/94/040605-07$03.00/0

MOLECULAR PHARMACOLOGY, 46:605-611, 1994.

Differential Induction of Etoposide-Mediated Apoptosis in Human Leukemia HL-60 and K562 Cells

MARY K. RITKE, JAMES M. RUSNAK, JOHN S. LAZO, WILLIAM P. ALLAN, CAROLINE DIVE, SUKBINDHER HEER, and JACK C. YALOWICH

Department of Pharmacology, University of Pittsburgh School of Medicine, Pittsburgh, Pennsylvania 15261 (M.K.R., J.M.R., J.S.L., W.P.A., J.C.Y.), and CRC Molecular and Cellular Pharmacology Group, School of Biological Sciences, University of Manchester, Manchester, M13 9PT England (C.D., S.H.)

Received May 4, 1994; Accepted July 8, 1994

SUMMARY

Etoposide (VP-16) is one of several DNA-damaging agents that induce subcellular structural changes associated with apoptosis. VP-16 exerts its DNA-damaging and cytotoxic effects subsequent to interference with DNA topoisomerase II activity. VP-16 also stimulates c-*jun* and c-*fos* mRNA expression in some cell lines, including human leukemia K562 and HL-60 cells. To compare the temporal relationship between drug-induced c-*jun* expression and apoptosis, we examined cell morphology, cell viability, DNA integrity, and c-*jun* induction during VP-16 treatment of K562 and HL-60 cells. VP-16 (10 μM)-induced internucleosomal DNA damage and nuclear fragmentation were readily apparent within 6 hr in HL-60 cells but were absent in K562 cells treated for up to 24 hr. Some internucleosomal DNA damage was observed in K562 cells but only after treatment with 100 μM VP-16 for 24 hr. In contrast, VP-16-induced DNA single-strand breaks, VP-16-induced topoisomerase II/DNA covalent complex formation, and VP-16-mediated growth inhibition were similar in K562 and HL-60 cells. Also, the time course of VP-16-induced c-*jun* mRNA expression was comparable for both K562 and HL-60 cell lines. Western blot analysis of whole-cell lysates showed that Bcl-2 protein levels were 13-fold greater in HL-60 cells than in K562 cells. Thus, the resistance of VP-16-treated K562 cells to apoptosis was not attributable to protection by Bcl-2. Furthermore, the relatively high levels of Bcl-2 in HL-60 cells were not sufficient to protect these cells against apoptosis. Together, our results indicate that the temporal coupling of VP-16-induced DNA damage, c-*jun* expression, and apoptosis is cell type specific and suggest that different signaling pathways for apoptosis are operating in these two human leukemia cell lines.

Topoisomerase II inhibitors exert cytotoxicity by inducing DNA single- and double-strand breaks (1). The DNA damage caused by topoisomerase II-inhibitory drugs such as amsacrine and the epipodophyllotoxins teniposide and VP-16 has two components (2, 3). First, these drugs stabilize a covalent topoisomerase II/DNA intermediate during strand passage, which prevents religation of cleaved DNA strands and subsequent enzyme turnover. The net result of this inhibitory function is the accumulation of protein-linked DNA strand breaks detectable by alkaline elution (4) or pulse field gel electrophoresis (2). The second component, which temporally follows the appearance of protein-linked DNA strand breaks in some cells, is more extensive DNA cleavage. In some cells, the resulting nucleosome-sized DNA ladders, detectable by conventional agarose gel electrophoresis (2, 3, 5), are typical of those seen in cells undergoing apoptosis (6).

Because changes in the levels of expression of some genes have been found to affect apoptosis (6–12), it has been suggested that a component of the orderly process of cell death is the coordinated expression of selected genes, particularly regulatory transcription factors. For example, several studies suggest a role for expression of the proto-oncogenes c-*fos* and c-*jun* in the regulation of apoptosis (8–12). Increased expression of these genes was observed after withdrawal of growth factors from interleukin-6- and interleukin-2-dependent lymphoid cells and before the appearance of nucleosomal ladders (8). Topoisomerase inhibitors also increased c-*fos* and c-*jun* expression in leukemia cell lines (10–12). Therefore, cytotoxic drug- and hormone-induced transcription of c-*fos* and c-*jun* suggests a signaling role for these genes in programmed cell death. This role is further supported by studies with antisense oligonucleotides to c-*fos* and c-*jun* that block apoptotic events associated with growth factor withdrawal (8).

This work was supported by American Cancer Society Grants DHP49 (J.C.Y.) and DHP77G (J.S.L.). M.K.R. is the recipient of a Pittsburgh Cancer Institute Postdoctoral Fellowship. J.M.R. is the recipient of a Pharmaceutical Manufacturer's Association Foundation Predoctoral Fellowship.

ABBREVIATIONS: VP-16, etoposide [4′-demethylepipodophyllotoxin-9-(4,6-*O*-ethylidene-β-D-glucopyranoside)]; β_2m, β_2-microglobulin; DMSO, dimethylsulfoxide; PAGE, polyacrylamide gel electrophoresis; PBS, phosphate-buffered saline; SDS, sodium dodecyl sulfate; topoisomerase II, DNA topoisomerase II (M_r 170,000 isoform); HEPES, 4-(2-hydroxyethyl)-1-piperazineethanesulfonic acid.

In contrast, another gene, *bcl-2*, has been assigned a protective role in apoptosis resulting from a wide variety of stimuli, including exposure to DNA-damaging agents (13). Fisher *et al.* (14) showed that Bcl-2 delays apoptosis, perhaps giving cells time to repair drug- or stress-induced DNA damage, generate mutations that increase oncogenic potential or drug resistance, and ultimately resume growth. Other evidence suggests that Bcl-2 expression may favor cell proliferation over apoptosis by increasing responsiveness to growth factors (15). Recently, proteins with significant homology to Bcl-2 (e.g., Bcl-X_L) that also protect cells against apoptosis have been identified (13, 16). An alternatively spliced variant of *bcl-x* (coding for Bcl-X_S) inhibits Bcl-2 function (13, 16). Additionally, proteins (for example, Bax) that bind to and block the protective effects of Bcl-2 have been characterized (17).

In this report we have studied VP-16-induced apoptosis in two human cell lines, the myeloid HL-60 cell line (18) and the chronic myelogenous leukemia cell line K562 (19). K562 cells (unlike HL-60 cells) contain the Philadelphia chromosome, a translocation characteristic of chronic myelogenous leukemia cells that fuses an unknown transcriptionally active region (bcr) with the c-*abl* proto-oncogene (20). The fusion of these two domains results in the constitutively activated Bcr/Abl tyrosine kinase (21).

We have compared the initial VP-16-induced DNA damage and the induction of c-*jun* expression with the onset of apoptosis in VP-16-treated K562 and HL-60 cells. Although cytotoxicity, initial DNA damage, VP-16-induced topoisomerase II/DNA covalent complex formation, and c-*jun* mRNA induction after VP-16 treatment were comparable for the two cell lines, apoptosis was readily apparent only in HL-60 cells. We also compared the expression of Bcl-2 in both cell lines and found that K562 cells expressed significantly lower levels of this protein than did HL-60 cells. Our data demonstrate that the protective effects of Bcl-2 and the temporal coupling of VP-16-induced DNA damage, transcription factor induction, and apoptosis are cell type specific, which suggests that the signaling pathways for apoptosis are distinct for these two human leukemia cell lines.

Materials and Methods

Cell lines. Human K562 cells were grown in suspension in Dulbecco's modified Eagle's medium supplemented with 10% fetal bovine serum and 2 mM L-glutamine. HL-60 cells were maintained in suspension in Iscove's modified Dulbecco's medium supplemented with 10% fetal bovine serum and 2 mM L-glutamine. Exponentially growing cells ($4–8 \times 10^5$ cells/ml) were used for all experiments.

Drugs and chemicals. VP-16 was obtained from Bristol-Myers Squibb (Wallingford, CT) and was dissolved in DMSO to prepare concentrated stock solutions (the final DMSO concentration in VP-16-treated and control cells was adjusted to 0.1%). Agarose was obtained from GIBCO/BRL (Bethesda, MD). Radiolabeled molecules were obtained from DuPont/NEN (Wilmington, DE). Unless otherwise indicated, all reagents were obtained from Sigma Chemical Co. (St. Louis, MO) or Fisher Scientific (Pittsburgh, PA).

Cell and nuclear staining. Plasma membrane integrity was assessed by staining 5×10^5 cells with trypan blue. Cells were collected by centrifugation ($2000 \times g$ for 5 min), resuspended in 20 μl of PBS, and stained by the addition of 20 μl of 0.4% trypan blue in PBS. The percentage of membrane-intact cells (not stained) was determined by counting five fields of >100 cells, using a hemocytometer. For analysis of nuclear morphology, 1×10^6 cells were pelleted and stained by resuspension in 10 μl of Hoechst 33342 solution (100 μM in PBS). Cells were incubated for 30 min before examininations with a Nikon Microphot-FX photomicroscope with an epifluorescence attachment.

Flow cytometry. VP-16 (10 or 100 μM) or DMSO (0.1%) was added to mid-logarithmic phase HL-60 and K562 cells (5×10^5/ml). At various times after drug addition (0–24 hr), 3×10^5 cells were collected, pelleted, washed with PBS, and resuspended in a final volume of 200 μl of ice-cold PBS. One milliliter of 70% (v/v) ethanol in PBS (equilibrated to −20°) was added to the resuspended cells with vigorous mixing. Fixed cells were incubated in the dark at 4° for 1–3 days. Cells were rehydrated in 300 μl of PBS for 25 min and then stained for 5 min with propidium iodide (final concentration, 16 μM) before flow analysis. Cells (10,000) were assessed with respect to their red fluorescence profile (575 ± 26 nm) using 488-nm excitation at 150 mW from a Coherent Enterprise laser of a FACS Vantage instrument (Becton Dickinson, San Jose, CA). Resulting DNA histograms were acquired using LYSIS II software (Becton Dickinson). Gates for the exclusion of debris were determined with the control samples (3 hr) and kept constant for all VP-16-treated samples. Quantitation of cell cycle distribution was determined with the CellFit program (SOBR model), which excludes DNA staining below the G_1 position. Two independent experiments were performed.

Internucleosomal DNA damage. The integrity of DNA from drug-treated and control cells was assessed by agarose gel electrophoresis. K562 (1×10^6) or HL-60 (2×10^6) cells were centrifuged for 30 sec in a TOMY HF120 Capsulefuge (Peninsula Laboratories, Belmont, CA). Cells were washed once with saline solution (0.85% NaCl), and the cell pellet was solubilized in 20 μl of lysis buffer (50 mM Tris·HCl, pH 8.0, 10 mM EDTA, 0.5% sodium laurylsarcosine, 0.5 mg/ml proteinase K). Pellets were incubated for 1 hr at 50°, after which 10 μl of 0.5 mg/ml RNase A were added. Samples were incubated for an additional 1 hr at 50° and heated to 70°, and 10 μl of molten 1% agarose in 10 mM EDTA, pH 8.0, were then added. The samples were loaded in dry wells of a 10- × 14-cm gel containing 2% agarose and 1× TPE (80 mM Tris, 2 mM EDTA, adjusted to pH 8.0 with phosphoric acid) and were electrophoresed at 40 V for 2 hr. Gels were stained for 30 min with 10 ng/ml ethidium bromide, destained for 30–60 min in water, and photographed with UV illumination.

Alkaline elution analysis of single-strand DNA damage. Drug-mediated DNA damage was assessed using the alkaline elution technique for high frequency single-strand breaks (4). K562 and HL-60 cells, which had been labeled for 48 hr with [2-^{14}C]thymidine (0.02 μCi/ml), were suspended at 5×10^5 cells/ml in buffer L (110 mM NaCl, 5 mM KCl, 1 mM $MgCl_2$, 5 mM NaH_2PO_4, 25 mM HEPES, 10 mM glucose) containing 0.1% DMSO or 2.5–20 μM VP-16 and were incubated for 60 min at 37°. K562 cells (5×10^6) containing [^{3}H]DNA were irradiated (1500 rad) on ice using a ^{137}Cs source (Mark Irradiator; J. L. Sheppard and Associates, Glendale, CA). These irradiated cells were added as internal standards to 7.5×10^5 drug-treated and ^{14}C-labeled K562 or HL-60 cells. After two washings in ice-cold PBS, cells were layered onto a polyvinyl chloride filter (pore size, 0.45 μm; Gelman Sciences, Ann Arbor, MI) and lysed with a solution of 2% SDS, 10 mM disodium EDTA, and 0.5 mg/ml proteinase K. The DNA was eluted from the filter with tetrapropylammonium hydroxide (Aldrich Chemicals, Milwaukee, WI), pH 12.1, at a flow rate of 0.16 ml/min, with a fractional interval of 5 min. The frequency of VP-16-induced DNA single-strand breaks was quantitated as the fraction of [^{14}C]DNA remaining on the filter when 75% of the ^{3}H-labeled internal standard DNA remained. A calibration curve relating the frequency of VP-16-induced DNA single-strand breaks to a corresponding effect of radiation (radiation equivalent DNA damage) using ^{14}C-labeled cells was obtained by plotting radiation dose (rads) versus [^{14}C]DNA retention at 75% retention of the [^{3}H]DNA internal standard.

Topoisomerase II/DNA binding assay. Topoisomerase II/DNA covalent complex formation in intact cells and nuclei was measured as described by Zwelling *et al.* (22). Briefly, K562 and HL-60 cells were prelabeled with [*methyl*-^{3}H]thymidine and [U-^{14}C]leucine for 24 hr, after which cells were treated for 1 hr with 10 μM VP-16 or 0.1% DMSO. Topoisomerase II/DNA complexes were isolated, and ^{3}H-

labeled DNA was quantitated relative to ^{14}C-labeled protein by scintillation counting of KCl/SDS precipitates.

Drug-induced growth inhibition. Exponentially growing K562 and HL-60 cells (5×10^5 cells/ml) were incubated with various concentrations of VP-16 (0.01–10 μM) or 0.1% DMSO for 3 hr. After exposure to drug, cells were washed twice with sterile PBS, counted using a ZBF Coulter counter (Coulter Electronics, Hialeah, FL), and resuspended to 1×10^5 cells/ml. The extent of growth beyond 1×10^5 cells/ml was determined after 48 hr and expressed as percentage inhibition of control growth. Replicate dose-response curves were used to calculate the 50% growth-inhibitory concentration for each cell line.

Expression of c-*jun*. Expression of c-*jun* mRNA expression was determined by Northern blot analysis after incubation of cells in the presence or absence of VP-16. Total RNA was extracted from guanidinium isothiocyanate lysates of $5–10 \times 10^6$ cells by acid-phenol extraction (23). RNA (10 μg) was electrophoresed through 1% agarose gels containing 0.3 M formaldehyde in 3-(*N*-morpholino)-propanesulfonic acid (24), transferred to Nytran nylon membranes (Schleicher and Schuell, Keene, NJ) by capillary blotting, and covalently fixed using an UV cross-linker (312 nm; 0.3 J/cm^2; Integrated Separations System, Natick, MA). The c-*jun* probe template was obtained by digesting the plasmid pJ1 (obtained from Dr. D. Bohmann, European Molecular Biology Laboratory, Heidelberg, Germany) with *Bam*HI and *Eco*RI (New England Biolabs, Beverly, MA) and isolating the 1.8-kilobase c-*jun* insert from low-melting point agarose gels. The 1.0-kilobase β_2m probe template was similarly isolated from plasmid pβ_2m (obtained from Dr. K. B. Tan, SmithKline Beecham, King of Prussia, PA) by digestion with *Pst*I. Probes were synthesized from ~30 ng of template DNA using the Klenow fragment of *Escherichia coli* DNA polymerase I (Boehringer Mannheim, Indianapolis, IN), [α-^{32}P] dCTP (300–3000 Ci/mmol), and random primer initiation (25). Probes were separated from unincorporated nucleotides using Sephadex G-50 spin columns, combined, and hybridized to Northern blots overnight by standard techniques (24). The c-*jun* and β_2m mRNAs were detected by autoradiography at −70° using Kodak XAR-5 X-ray film (Rochester, NY) and were quantitated by scanning densitometry using an LKB model 2222 laser densitometer and GSXL software (LKB-Pharmacia, Piscataway, NJ).

Western blot analysis of Bcl-2. Lysates were prepared from 5×10^6 cells by dissolving cell pellets in SDS-PAGE sample buffer (0.125 M Tris·HCl, pH 6.8, 2% SDS, 1 M urea, 10% glycerol, 5% β-mercaptoethanol). Lysates were sonicated to reduce viscosity, and 1–10 μg of protein were loaded in each well of a 12% SDS-PAGE gel. Resolved proteins were electrophoretically transferred to nitrocellulose and incubated sequentially with anti-human Bcl-2 monoclonal antibody (Dako Corp., Carpinteria, CA) and horseradish peroxidase-conjugated goat anti-mouse IgG (Upstate Biotechnologies, Lake Placid, NY). Bound antibodies were detected using enhanced chemiluminescence (Amersham Life Sciences, Arlington Heights, IL). Autoradiographic signals were quantitated by densitometric scanning using an LKB laser densitometer (LKB-Pharmacia).

Results

Cell viability and nuclear morphology. Both K562 and HL-60 cells remained >90% membrane-intact for up to 24 hr after treatment with 10 μM VP-16, as determined by the ability to exclude trypan blue dye (Table 1). By 48 hr after drug addition, no intact HL-60 cells remained. K562 cells treated with 10 μM VP-16 for up to 96 hr or 100 μM VP-16 for 24 hr also maintained >95% viability (data not shown). After 72 hr in the presence of 100 μM VP-16, <50% of K562 cells remained (the rest were cell debris), of which only 75% excluded trypan blue. By 96 hr after drug addition, all of the 100 μM VP-16-treated K562 cells appeared dead. Finally, K562 and HL-60 cells were exposed for 3 hr to various concentrations of VP-16 and cell growth was assessed 48 hr later. The VP-16-mediated 50% growth-inhibitory concentrations for K562 and HL-60 cells were comparable (2.4 ± 0.7 μM and 1.4 ± 1.0 μM, respectively; mean ± standard error from three experiments; $p = 0.34$, Student's *t* test). Collectively, these data and previous results demonstrating that a 1-hr incubation with VP-16 (10 μM) reduced K562 cell colony formation by 85% (26) indicate that VP-16 is cytocidal to both HL-60 cells and K562 cells. Clearly, cytoplasmic membrane disruption (as assessed by trypan blue staining) was significantly delayed in K562 cells, compared with HL-60 cells.

TABLE 1

Trypan blue exclusion in K562 and HL-60 cells

Results are mean ± standard error of three to five independent experiments.

Cell Line	Time	Trypan Blue-Positive Cells	
		0.1% DMSO	+10 μM VP-16
	hr	%	
K562	14	2.6 ± 1.0	1.6 ± 0.3
	24	1.3 ± 0.4	4.2 ± 0.7
HL-60	14	1.3 ± 0.4	2.5 ± 0.8
	24	4.1 ± 1.3	9.0 ± 4.3

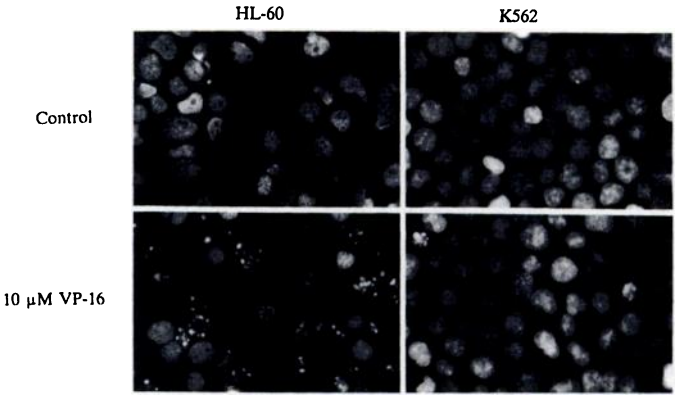

Fig. 1. Fluorescent micrographs of 0.1% DMSO- or 10 μM VP-16-treated HL-60 and K562 cells. After 6 hr of exposure to DMSO or VP-16, 1×10^6 cells were stained with 0.1 mM Hoechst 33342.

Hoechst 33342 staining of cells after a 6-hr drug exposure revealed extensive nuclear condensation and fragmentation, as well as the appearance of apoptotic bodies in HL-60 cells treated with 10 μM VP-16 (Fig. 1, *left*). In contrast, 10 μM VP-16-treated K562 cells and nuclei remained morphologically indistinguishable from control cells (Fig. 1, *right*). The percentage of apoptotic cells (with fragmented nuclei) was quantitated for cells treated for 6 or 24 hr with 10 μM VP-16 or 0.1% DMSO. The results from three separate experiments are summarized in Fig. 2. Six hours after drug addition, 35% of HL-60 nuclei were observed to be apoptotic; after 24 hr, 90% of HL-60 cells in the presence of VP-16 exhibited apoptotic morphology. In contrast, VP-16-treated K562 cells (6–24 hr) remained morphologically indistinguishable from control (DMSO-treated) cells.

Flow cytometry of VP-16-treated cells. VP-16 (10 μM)- and DMSO (0.1%)-treated K562 and HL-60 cells were stained with propidium iodide, and cell cycle distribution was analyzed by flow cytometry. The profiles of the DNA histograms were strikingly different for untreated HL-60 and K562 cells (Fig. 3). HL-60 cells exhibited a sharp G_0/G_1 peak and clearly distinguishable S and G_2/M phases (Fig. 3A). In contrast, K562 cells

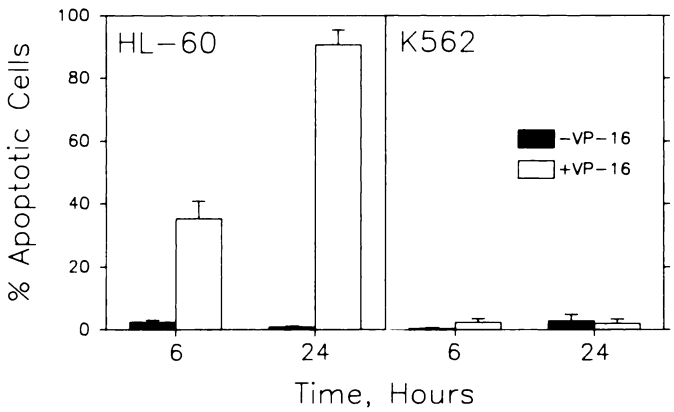

Fig. 2. Accumulation of apoptotic cells in HL-60 and K562 cell cultures treated for 6 or 24 hr with 0.1% DMSO (■) or 10 μM VP-16 (□). Cells (1 × 10^6) were stained with Hoechst 33342 as in Fig. 1. For each experiment, at least 100 cells from at least two fields were counted in duplicate. *Bars*, mean ± standard error from three separate experiments performed on separate days.

(which are aneuploid) showed a much broader distribution with no clearly distinguishable G_0/G_1, S, or G_2/M phases, consistent with the variable chromosome number of these cells (Fig. 3B). The addition of VP-16 had differing effects on the subsequent DNA histogram profiles. For HL-60 cells, the first detectable drug-induced change in cell cycle distribution was seen 6 hr after addition of 10 μM VP-16, with a dramatic decrease in the number of cells in S and G_2/M phases (Fig. 3C). Although mitotic cells are most sensitive to VP-16 (27), apoptosis occurred so rapidly that an accumulation of cells at G_2/M was not observed in flow histograms of HL-60 cells (Fig. 3C). Similar results were also reported for VP-16-treated thymocytes, teniposide-treated HL-60 cells, and VP-16-treated CEM cells (2, 28, 29). The appearance of HL-60 cells with subdiploid DNA (note the shoulder to the left of G_1 in Fig. 3C) is indicative of the accumulation of apoptotic nuclei (29–31). In contrast to HL-60 cells, the DNA histograms of K562 cells treated with 10 μM VP-16 for 6 hr (Fig. 3D) or 12–24 hr (data not shown) were indistinguishable from those of 0.1% DMSO-treated K562 cells. Similar profiles were seen with K562 cells treated for 6 hr with 100 μM VP-16 (data not shown). Together, these results indicate rapid VP-16-induced apoptosis in HL-60 cells but not in K562 cells.

Internucleosomal DNA damage in VP-16-treated cells. DNA was prepared from 1–2 × 10^6 K562 or HL-60 cells that had been treated for 3, 6, or 24 hr with 10 or 100 μM VP-16. The integrity of the DNA was assessed by agarose gel electrophoresis (Fig. 4). Internucleosomal DNA damage in HL-60 cells was readily detected 6 hr after treatment with 10 μM VP-16 or 3 hr after treatment with 100 μM VP-16. By 24 hr after drug addition, DNA damage was so severe that ladders were obscured by an unresolved smear. In contrast, the DNA from K562 cells remained intact under all conditions except 24-hr treatment with 100 μM VP-16. Even after 24 hr of VP-16 treatment, the laddering was not extensive in K562 cells (Fig. 4, *rightmost lane*). In addition, no extensive DNA laddering was observed in K562 cells treated for 24–72 hr with 10–100 μM VP-16 (data not shown). These results demonstrate the resistance of K562 cells to VP-16-induced apoptosis. In separate experiments, a 6-hr incubation of both K562 and HL-60 cells with teniposide (10 μM), amsacrine (10 μM), or nitrogen mustard (30 μM) resulted in internucleosomal DNA damage only in HL-60 cells (data not shown). These results further demonstrate that K562 cells are refractory to drug-induced apoptosis, compared with HL-60 cells.

VP-16-induced-DNA damage and topoisomerase II/DNA covalent binding. Alkaline elution analysis of initial DNA damage in K562 and HL-60 cells treated for 60 min with various concentrations of VP-16 showed similar concentration-dependent accumulation of DNA single-strand breaks for both cell lines (Fig. 5). Also, SDS/KCl precipitation of cell lysates from VP-16-treated (1 hr) K562 and HL-60 cells revealed comparable concentration-dependent accumulation of drug-induced topoisomerase II/DNA covalent complexes (Fig. 6). These results indicate that the initial cytotoxic effects of VP-16 (DNA damage, drug-stabilized topoisomerase II binding to DNA, and inhibition of cell growth) are comparable for both leukemic cell lines.

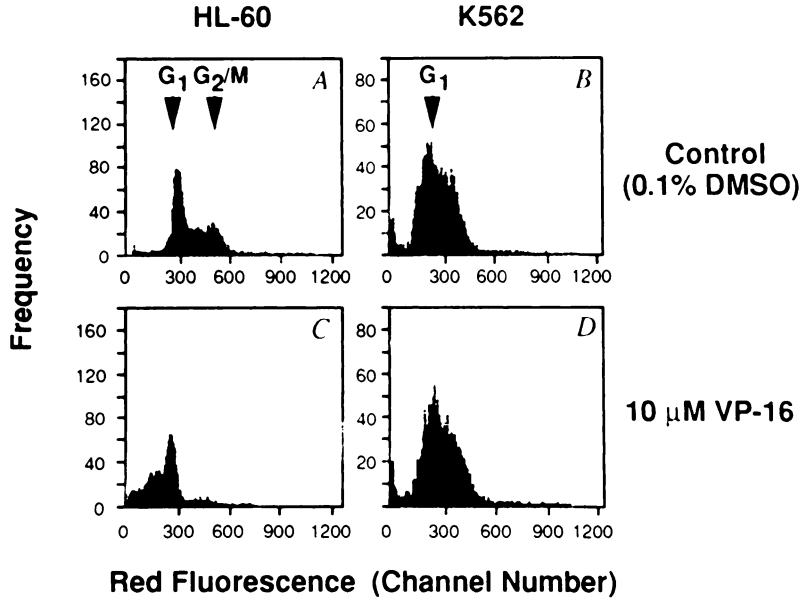

Fig. 3. Flow cytometric analysis of HL-60 (A and C) and K562 (B and D) cells treated for 6 hr with 0.1% DMSO (A and B) or 10 μM VP-16 (C and D). Ethanol-fixed cells (10,000) were stained with 16 μM propidium iodide before sorting. Debris was excluded (by gating a control sample) from analysis. Shown are representative histograms from one of two experiments.

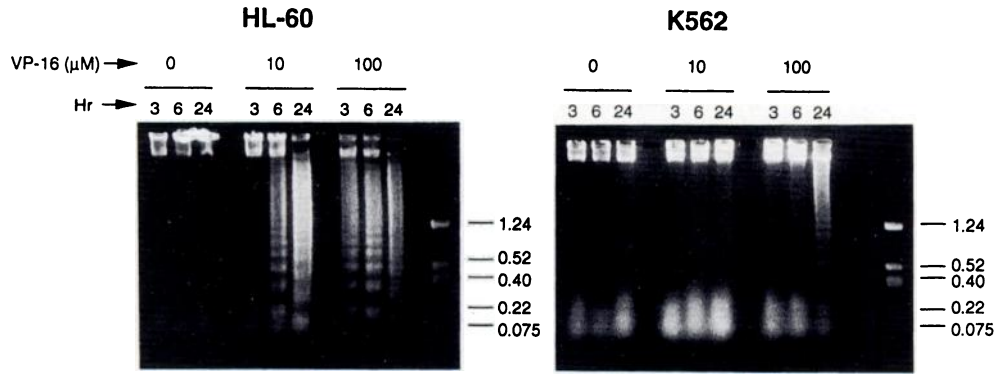

Fig. 4. Internucleosomal DNA fragmentation in HL-60 and K562 cells treated with 0–100 μM VP-16 for 3–24 hr. DNA from 5 × 10^6 HL-60 or 2.5 × 10^6 K562 cells was electrophoresed through 2% agarose gels and stained with 10 ng/ml ethidium bromide. *Numbers to the right of the gels*, sizes of *HinfI*-digested pSP65 DNA fragments.

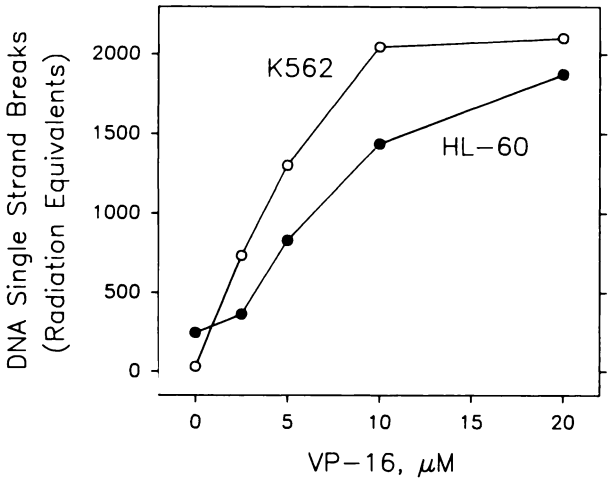

Fig. 5. DNA single-strand breaks in K562 and HL-60 cells treated for 1 hr in the presence 0–20 μM VP-16. A calibration curve relating the frequency of VP-16-induced single-strand breaks to a corresponding effect of equivalent radiation-induced DNA damage was obtained by plotting radiation dose (rads) versus [^{14}C]DNA retention at 75% retention of the [^{3}H]DNA internal standard.

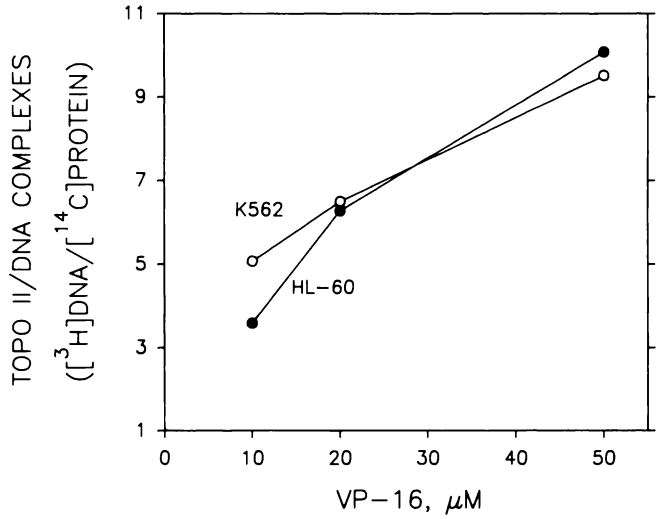

Fig. 6. Topoisomerase II/DNA covalent complex formation in K562 and HL-60 cells treated for 1 hr with 10 μM VP-16. Cells were prelabeled for 24 hr with [*methyl*-^{3}H]thymidine and [U-^{14}C]leucine and then incubated in the presence of 0.04% DMSO or 10 μM VP-16. Topoisomerase II/DNA covalent complexes were isolated by KCl/SDS precipitation and were quantitated by scintillation counting. The results shown, expressed as the ^{3}H/^{14}C (cpm) ratio of VP-16-induced covalent complexes, were corrected for background levels by subtraction of counts precipitated in DMSO-treated cells.

Induction of c-*jun* by VP-16. Because c-*jun* mRNA expression is increased by DNA damage and because c-*jun* is a candidate in apoptotic signaling (8–12), we examined the effects of VP-16 on c-*jun* expression. K562 and HL-60 cells were exposed for 0–12 hr to 200 or 100 μM VP-16, respectively. Under these conditions, 95% of cells excluded trypan blue. The drug concentrations used for this kinetic study were selected to yield maximum induction of c-*jun* mRNA, based on previous results (32). At various times after drug addition, RNA was isolated and c-*jun* mRNA expression was measured by Northern blot analysis. Levels of c-*jun* mRNA were normalized to that of the internal control β_2m mRNA, levels of which remained relatively constant for up to 12 hr after drug addition (data not shown). The results of two or three experiments (expressed as fold increase of c-*jun* levels in drug-treated cells, compared with 0.1% DMSO-treated cells) are summarized in Fig. 7. VP-16 stimulated c-*jun* by >8-fold in K562 cells and up to 5.5-fold in HL-60 cells, with peak levels being attained 2.5–3 hr after drug addition. Levels of c-*jun* returned to nearly basal levels by 12 hr after drug addition. Thus, there was no clear correlation between induction of c-*jun* expression (Fig. 7) and the onset of apoptosis (Fig. 4).

Expression of Bcl-2. Western blot analysis of HL-60 and K562 whole-cell lysates (1–10 μg of protein) revealed a prominant 26-kDa Bcl-2 band in HL-60 cell lysates (Fig. 8, *left two lanes*). In contrast, K562 cells showed markedly less Bcl-2, compared with HL-60 cells (Fig. 8, *right lane*). The Bcl-2 densitometric signal (area under the scanned peak) obtained with various amounts of HL-60 cell protein served as a standard curve from which Bcl-2 signals for K562 cells were quantitated. Densitometric scanning of three independent Western blots containing various quantities of HL-60 (1–10 μg) and K562 (10–20 μg) lysates revealed that HL-60 cells contained 13.4 ± 2.5-fold (mean ± standard error) more Bcl-2 protein than did K562 cells.

Discussion

Our study dissociates induction of c-*jun* expression and the appearance of apoptosis in K562 cells, as defined by either the electrophoretic detection of internucleosomal DNA fragmen-

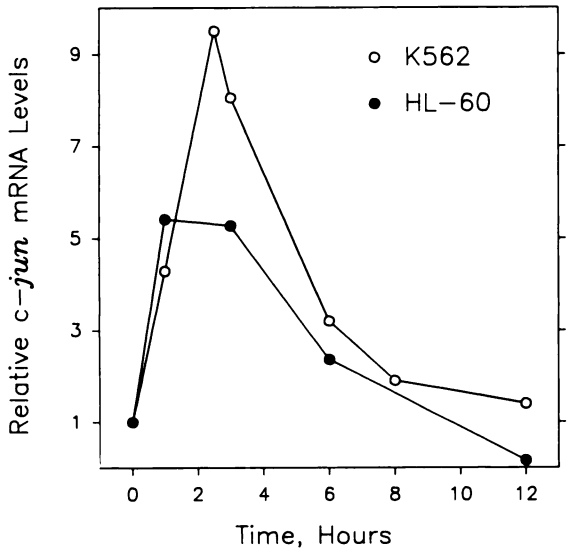

Fig. 7. Stimulation of c-*jun* mRNA expression in VP-16-treated K562 and HL-60 cells. Total RNA was isolated, at the times indicated, from cells treated with 200 μM (K562) or 100 μM (HL-60) VP-16. RNA (10 μg) was analyzed by Northern blotting and hybridization to ^{32}P-labeled probes for c-*jun* and β_2m, as described in Materials and Methods. Data points presented are the mean of two or three independent experiments; the range or standard error for each data point was <15%.

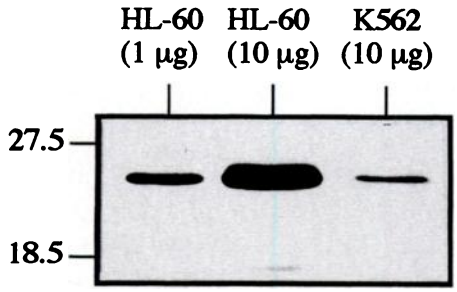

Fig. 8. Levels of Bcl-2 in HL-60 and K562 cells. Cell lysates (1–10 μg of protein) were electrophoresed by SDS-PAGE and Western blotted to nitrocellulose. The Bcl-2 was labeled by sequential incubation with monoclonal antibody to human Bcl-2 and horseradish-conjugated goat anti-mouse IgG. Bound antibodies were detected by enhanced chemiluminescence. *Numbers to the left of the blot*, positions of molecular mass markers (in kDa).

tation (Fig. 4) or the appearance of apoptotic bodies (Figs. 1 and 2). Using the appearance of fragmented nuclei (Fig. 1) as a criterion, we observed no sign of apoptosis up to 24 hr after continuous treatment of K562 cells with relatively high concentrations of VP-16 (Fig. 2). HL-60 cells with subdiploid DNA (distinguishable from cell debris) were noted 6 hr after addition of 10 μM VP-16 (Fig. 3). In contrast, reduced staining of K562 DNA was observed only after a 24-hr exposure to 100 μM VP-16, and not to the same extent as for HL-60 cells (data not shown).

Several groups have provided data that support a role for c-*jun* in apoptosis (8, 10–12). In this study we compared the time course of VP-16-mediated c-*jun* induction for K562 and HL-60 cells. Induction of c-*jun* expression in response to 100 μM VP-16 was similar for both cell lines (Fig. 7). However, only HL-60 cells readily showed subsequent evidence of apoptosis (Fig. 4). In addition, the concentrations of VP-16 necessary to maximally stimulate c-*jun* mRNA (100 μM) and to achieve apoptosis (10 μM) in HL-60 cells were significantly different. We observed no overexpression of c-*jun* mRNA in HL-60 cells incubated for up to 6 hr with 10 μM VP-16 (data not shown), in contrast to results reported by another group (12). Hence, in our laboratories the induction of c-*jun* by VP-16 is clearly not required to initiate apoptosis in HL-60 cells.

The signaling systems that couple initial DNA damage with the apoptotic response appear complex and have not been fully characterized. Bcl-2 has been assigned a protective role in apoptosis resulting from a wide variety of stimuli, including exposure to DNA-damaging agents (13–15). Paradoxically, K562 cells, which are refractory to apoptosis, compared with HL-60 cells, exhibit significantly less Bcl-2 protein than do HL-60 cells (Fig. 8). We cannot exclude the possibility that HL-60 cells express a defective Bcl-2 recognized by our antibody or that HL-60 cells contain high levels of a Bcl-2-binding and -inactivating protein, such as Bax. Another mechanism for regulation of apoptosis has been proposed from the studies of Barry *et al.* (33), which demonstrated that reduction of intracellular pH in HL-60 cells is associated with apoptosis, consistent with conditions required for activation of an endonuclease. Multiple intracellular nucleases with potential involvement in apoptosis may exist (34). Thus, HL-60 cells may contain a monocytic/granulocytic endonuclease that is limiting, inactive, or absent in K562 cells and other erythroid/myeloid lineage cell lines.

The relatively low levels of Bcl-2 and the significant delay of VP-16-induced apoptosis in K562 cells, compared with HL-60 cells, suggest that K562 cells may express a functional Bcl-2 homologue. K562 cells, unlike HL-60 cells, constitutively express an activated Bcr/Abl tyrosine kinase (21). Recently, the expression of transfected v-*abl* or Bcr/Abl was shown to suppress apoptosis induced by growth factor deprivation or by drug treatments, including VP-16 (35–38). Therefore, the results presented in this study are consistent with the current hypothesis that Abl tyrosine kinase activity serves a function analgous to that of Bcl-2, i.e., to suppress drug-induced apoptosis.

The process of apoptosis most likely involves initial (drug-target interaction) and late (nucleosomal fragmentation) events (14, 39, 40). The involvement of gene products from c-*jun*, c-*fos*, and *bcl-2* is likely to occur in the signal pathway(s) between these initial and late events. Our results suggest that in VP-16-treated cells c-*jun* induction, like drug-induced accumulation of covalent topoisomerase II/DNA complexes and DNA strand breaks, is most closely associated with an early event that precedes apoptotic signaling pathways in some cells, such as HL-60 cells. It is clear from other studies that Bcl-2 protection of cells from apoptosis is distal to the drug-target interaction (14, 39). However, the presence of high levels of Bcl-2 in HL-60 cells indicates that this protein alone cannot delay apoptosis in all cells. Thus, additional factors can supercede Bcl-2 function in cells. The marked delay or absence of typical apoptotic processes after VP-16 treatment in K562 cells suggests that caution is needed in assigning universal roles for the expression of c-*jun*, *bcl-2*, and other genes and their products in all hematopoietic cells. The results of our study highlight the need to identify additional biochemical pathways and indicators of cell death for cells, like K562, that are refractory to apoptosis.

References

1. Liu, L. F. DNA topoisomerase poisons as antitumor drugs. *Annu. Rev. Biochem.* 58:351–377 (1989).
2. Walker, P. R., C. Smith, T. Youdale, J. Leblanc, J. F. Whitfield, and M.

Sikorska. Topoisomerase II-reactive chemotherapeutic drugs induce apoptosis in thymocytes. *Cancer Res.* **51**:1078–1085 (1991).
3. Kaufmann, S. H. Induction of endonucleolytic DNA cleavage in human acute myelogenous leukemia cells by etoposide, camptothecin, and other cytotoxic anticancer drugs: a cautionary note. *Cancer Res.* **49**:5870–5878 (1989).
4. Kohn, K. W., L. C. Erickson, R. A. G. Ewig, and C. A. Friedman. Fractionation of DNA from mammalian cells by alkaline elution. *Biochemistry* **15**:4629–4637 (1976).
5. Hotz, M. A., F. Traganos, and Z. Darzynkiewicz. Changes in nuclear chromatin related to apoptosis or necrosis induced by the DNA topoisomerase II inhibitor fostriecin in MOLT-4 and HL-60 cells are revealed by altered DNA sensitivity to denaturation. *Exp. Cell Res.* **201**:184–191 (1992).
6. Wyllie, A. H. Apoptosis. *Br. J. Cancer* **67**:205–208 (1993).
7. Wyllie, A. H., R. G. Morris, A. L. Smith, and D. Dunlop. Chromatin cleavage in apoptosis: association with condensed chromatin morphology and dependence on macromolecular synthesis. *J. Pathol.* **142**:67–77 (1984).
8. Colotta, F., N. Polentarutti, M. Sironi, and A. Mantovani. Expression and involvement of c-*fos* and c-*jun* protooncogenes in programmed cell death induced by growth factor deprivation in lymphoid cell lines. *J. Biol. Chem.* **267**:18278–18283 (1992).
9. Andrews, G. K., M. A. Harding, J. P. Calvet, and E. D. Adamson. The heat shock response in HeLa cells is accompanied by elevated expression of the c-*fos* proto-oncogene. *Mol. Cell. Biol.* **7**:3452–3458 (1987).
10. Hollander, M. C., and A. J. Fornace, Jr. Induction of *fos* RNA by DNA-damaging agents. *Cancer Res.* **49**:1687–1692 (1989).
11. Kharbanda, S., E. Rubin, H. Gunji, H. Hinz, B. Giovanella, P. Pantazis, and D. Kufe. Camptothecin and its derivatives induce expression of the c-*jun* protooncogene in human myeloid leukemia cells. *Cancer Res.* **51**:6636–6642 (1991).
12. Rubin, E., S. Kharbanda, H. Gunji, and D. Kufe. Activation of the c-*jun* protooncogene in human myeloid leukemia cells treated with etoposide. *Mol. Pharmacol.* **39**:697–701 (1991).
13. Reed, J. *Bcl*-2 and the regulation of programmed cell death. *J. Cell Biol.* **124**:1–6 (1994).
14. Fisher, T. C., A. E. Milner, C. D. Gregory, A. L. Jackman, G. W. Aherne, J. A. Hartley, C. Dive, and J. A. Hickman. *Bcl*-2 modulation of apoptosis induced by anticancer drugs: resistance to thymidylate stress is independent of classical resistance pathways. *Cancer Res.* **53**:3321–3326 (1993).
15. Reed, J. C., H. S. Talwar, M. Cuddy, G. Baffy, J. Williamson, U. R. Rapp, and G. J. Fisher. Mitochondrial protein $p26^{bcl2}$ reduces growth factor requirements of NIH3T3 fibroblasts. *Exp. Cell Res.* **119**:277–283 (1991).
16. Boise, L. H., M. Gonzalez-Garcia, C. E. Postema, L. Ding, T. Lindstein, L. A. Turka, X. Mao, G. Nunez, and C. Thompson. *Bcl-x*, a *bcl*-2-related gene that functions as a dominant regulator of apoptotic cell death. *Cell* **74**:597–608 (1993).
17. Oltvai, Z. N., C. L. Milliman, and S. J. Korsmeyer. Bcl-2 heterodimerizes *in vivo* with a conserved homolog, BAX, that accelerates programmed cell death. *Cell* **74**:609–619 (1993).
18. Dalton, W. T., M. J. Ahearn, K. B. McCredie, E. J. Freireich, S. A. Stass, and J. M. Trujillo. HL-60 cell line was derived from a patient with FAB-M2 and not FAB-M3. *Blood* **71**:242–247 (1988).
19. Lozzio, B., and C. Lozzio. Properties and usefulness of the original K-562 human myelogenous leukemia cell line. *Leuk. Res.* **3**:363–370 (1979).
20. Collins, S. J., and M. T. Groudine. Rearrangement and amplification of c-*abl* sequences in the human chronic myelogenous leukemia cell line K562. *Proc. Natl. Acad. Sci. USA* **80**:4813–4817 (1983).
21. Konpka, J. B., and O. N. Witte. Detection of c-*abl* tyrosine kinase activity *in vitro* permits direct comparison of normal and altered *abl* gene products. *Mol. Cell. Biol.* **5**:3116–3123 (1985).
22. Zwelling, L. A., M. Hinds, D. Chan, J. Mayes, K. Lan Sie, E. Parker, L. Silberman, A. Radcliffe, M. Beran, and M. Blick. Characterization of an amsacrine-resistant line of human leukemia cells: evidence for a drug-resistant form of topoisomerase II. *J. Biol. Chem.* **264**:16411–16420 (1989).
23. Chomczynski, P., and N. Sacchi. Single-step method of RNA isolation by acid guanidinium thiocyanate-phenol-chloroform extraction. *Anal. Biochem.* **162**:156–159 (1987).
24. Maniatis, T., E. F. Fritsch, and J. Sambrook. *Molecular Cloning: A Laboratory Manual.* Cold Spring Harbor Laboratory, Cold Spring Harbor, NY, 187–210 (1982).
25. Feinberg, A. P., and B. Vogelstein. A technique for radiolabeling DNA restriction fragments to high specific activity. *Anal. Biochem.* **137**:266–267 (1983).
26. Yalowich, J. C., J. R. Zucali, M. A. Gross, and W. E. Ross. Effects of verapamil on etoposide, vincristine, and Adriamycin activity in normal human bone marrow granulocyte-macrophage progenitors and in human K562 leukemia cells *in vitro*. *Cancer Res.* **45**:4921–4924 (1985).
27. Estey, E., R. C. Adlakha, W. H. Hittelman, and L. A. Zwelling. Cell cycle stage dependent variations in drug-induced topoisomerase II mediated DNA cleavage and cytotoxicity. *Biochemistry* **26**:4338–4344 (1987).
28. DelBino, G., and Z. Darzynkiewicz. Camptothecin, teniposide, or 4′-(9-acridinylamino)-3-methanesulfon-*m*-anisidide, but not mitoxantrone or doxorubicin, induces degradation of nuclear DNA in S phase of HL-60 cells. *Cancer Res.* **51**:1165–1169 (1991).
29. Catchpoole, D. R., and B. W. Stewart. Etoposide-induced cytotoxicity in two human T-cell leukemic lines: delayed loss of membrane permeability rather than DNA fragmentation as an indicator of programmed cell death. *Cancer Res.* **53**:4287–4296 (1993).
30. Nicoletti, I., G. Migliorati, M. C. Pagliacci, F. Grignani, and C. Riccardi. A rapid and simple method for measuring thymocyte apoptosis by propidium iodide staining and flow cytometry. *J. Immunol. Methods* **139**:271–279 (1991).
31. Darzynkiewicz, Z., S. Bruno, G. del Bino, W. Gorczyca, M. A. Hotz, P. Lassota, and F. Traganos. Features of apoptotic cells measured by flow cytometry. *Cytometry* **13**:795–808 (1992).
32. Ritke, M. K., V. V. Bergoltz, W. P. Allan, and J. C. Yalowich. Increased c-*jun*/AP-1 levels in etoposide resistant human leukemia K562 cells. *Biochem. Pharmacol.* **48**:525–533 (1994).
33. Barry, M. A., J. E. Reynolds, and A. Eastman. Etoposide-induced apoptosis in human HL-60 cells is associated with intracellular acidification. *Cancer Res.* **53**:2349–2357 (1993).
34. Eastman, A., and M. A. Barry. The origins of DNA breaks: a conseqeuence of DNA damage, DNA repair, or apoptosis? *Cancer Invest.* **10**:229–240 (1992).
35. Evans, C. A., P. J. Owen-Lynch, A. D. Whetton, and C. Dive. Activation of the Abelson tyrosine kinase activity is associated with suppression of apoptosis in hemopoietic cells. *Cancer Res.* **53**:1735–1738 (1993).
36. Chapman, R. S., A. D. Whetton, and C. Dive. The suppression of drug-induced apoptosis by activation of v-ABL protein tyrosine kinase. *Cancer Res.* **54**:5131–5137 (1994).
37. Laneuville, P., M. Timm, and A. T. Hudson. Bcr/abl expression in 32D c13(G) cells inhibits apoptosis induced by protein tyrosine kinase inhibitors. *Cancer Res.* **54**:1360–1366 (1994).
38. McGahon, A., R. Bissonnette, M. Schmitt, K. M. Cotter, D. R. Green, and T. G. Cotter. BCR-ABL maintains resistance of chronic myelogenous leukemia cells to apoptotic cell death. *Blood* **83**:1179–1187 (1994).
39. Kamesaki, S., H. Kamesaki, T. J. Jorgensen, A. Tanizawa, Y. Pommier, and J. Cossman. BCL-2 protein inhibitis etoposide-induced apoptosis through its effects on events subsequent to topoisomerase II-induced DNA strand breaks and their repair. *Cancer Res.* **53**:4251–4256 (1993).
40. Dive, C., and J. A. Hickman. Drug-target interactions: only the first step in the commitment to a programmed cell death? *Br. J. Cancer* **64**:191–196 (1991).

Send reprint requests to: Jack C. Yalowich, Department of Pharmacology, University of Pittsburgh School of Medicine, W1308 Biomedical Sciences Tower, Pittsburgh, PA 15261.